

## ORIGINAL RESEARCH ARTICLE

# One-pot synthesis of triazole and oxadiazoline derivatives from naproxen: A sustainable approach in green chemistry

Naghm Majid Abdulhassan\*, Abdull Jabar Attia, Falah S. Al-Fartusie

Chemistry Department, College of Science, Mustansiriyah University, Baghdad, 10052, Iraq

\*Corresponding author: Naghm Majid Abdulhassan, naghamejed@uomustansiriyah.edu.iq

## ABSTRACT

This study presents a novel, one-pot synthetic strategy for preparing triazole and oxadiazoline derivatives directly from naproxen. This approach aligns with the principles of green chemistry, aiming to enhance synthetic efficiency by minimizing reaction steps and reducing waste. By eliminating the need for multiple isolation and purification stages, this method offers a sustainable alternative to conventional multi-step procedures. The synthesized compounds underwent structural confirmation using a suite of spectroscopic techniques, specifically Fourier-Transform Infrared spectroscopy, Proton Nuclear Magnetic Resonance spectroscopy, and Carbon-13 Nuclear Magnetic Resonance spectroscopy and CNMR dept 135 and CNMR dept 90. Further analysis supported their potential as anti-inflammatory agents through molecular docking studies. These studies demonstrated strong binding affinities of the compounds to the cyclooxygenase-2 (COX-2) enzyme, suggesting a favorable mechanism of action for anti-inflammatory activity. Additionally, their acute toxicity was assessed by determining the LD50 values, providing preliminary data on their safety profile. Collectively, the new derivatives exhibited promising multi-target activity. The synthesized compounds exhibit potent broad-spectrum antimicrobial effects, demonstrating significant efficacy against both "Gram-positive bacteria, *Staphylococcus aureus* and *Staphylococcus epidermidis*", and "Gram-negative bacteria, including *Klebsiella* species and *Escherichia coli*". Furthermore, they show promising antifungal activity against the pathogenic yeast *Candida albicans*". This research demonstrates that a sustainable, one-pot synthesis can efficiently generate new compounds with valuable biological properties. Sustained-release naproxen derivatives show significant potential for future development in medicinal chemistry. This work highlights the constructive collaboration between green chemistry principles and the discovery of novel therapeutic agents.

**Keywords:** naproxen; triazole; oxadiazoline; One-Pot Synthesis; green chemistry; LD50, medicinal chemist

## ARTICLE INFO

Received: 6 November 2025

Accepted: 8 December 2025

Available online: 05 January 2026

## COPYRIGHT

Copyright © 2026 by author(s).

Applied Chemical Engineering is published by Arts and Science Press Pte. Ltd. This work is licensed under the Creative Commons Attribution-NonCommercial 4.0 International License (CC BY 4.0).

<https://creativecommons.org/licenses/by/4.0/>

## Graphical abstract



## 1. Introduction

Green chemistry is a modern scientific methodology that focuses on designing chemical products and processes in a sustainable way<sup>[1,2]</sup>. This field goes beyond simply treating pollution; it aims to prevent pollution at its source<sup>[3,4]</sup> by reducing or eliminating the use and generation of substances that pose a risk to the environment or human health<sup>[1,5]</sup>. To ensure chemical sustainability throughout the entire lifecycle of a substance, including manufacturing and final disposal<sup>[3,5]</sup>. "The Twelve Principles of Green Chemistry were developed by Paul Anastas and John Warner in the late 1990s"<sup>[6,7]</sup>. These principles form a structured guiding framework that directs chemical processes toward safer alternatives with a lower environmental impact<sup>[8,9]</sup>. These principles encompass several key areas, such as waste reduction, increased atom economy, less toxic reaction design, the use of renewable raw materials, reduced energy consumption, and continuous process monitoring to reduce risks<sup>[10,11]</sup>. These principles form the basis for developing sustainable chemical processes that help protect the environment and promote a circular economy<sup>[12,13]</sup>.

One-pot synthesis is a chemical technique in which multiple reaction steps are performed sequentially within a single reaction vessel without the need for breaks or cleanup between steps<sup>[14,15]</sup>. This approach offers several advantages that make it one of the most important green chemistry strategies<sup>[16,17]</sup>. Reduced solvent and chemical consumption: In traditional methods, the reaction requires transferring materials from one vessel to another with each reaction step, consuming more solvents and reagents<sup>[18]</sup>. In one-pot synthesis, all steps are performed in a single vessel without the need for repeated separation and purification, reducing the use of harmful chemicals and solvents<sup>[19]</sup>. Reduced chemical waste: By reducing separation and purification steps and using the same vessel, the production of chemical waste and organic waste is reduced, contributing to a reduced environmental impact of the process<sup>[20-22]</sup>. A single reaction in a single vessel saves time spent cleaning and preparing between steps and reduces the need for repeated heating or cooling, resulting in reduced energy consumption, and is typically designed to produce larger quantities of the desired product at a higher rate than the overall reaction, making the process more economical and efficient compared to methods that involve multiple separation and purification steps<sup>[23,24]</sup>. Simplifying the process and reducing health and safety risks, the handling of chemicals in multiple steps contributes to reducing chemists' exposure to toxic or flammable materials, making the process safer<sup>[25,26]</sup>.

These features make one-pot synthesis a practical example of applying green chemistry principles and a sustainable strategy for reducing the environmental impacts associated with chemical manufacturing. In this context, naproxen, a widely used nonsteroidal anti-inflammatory drug (NSAID), is a promising raw material for synthesizing new compounds with medical value<sup>[27,28]</sup>. The synthesis of triazole and oxadiazine derivatives from naproxen is not only an addition to the library of organic compounds, but it also opens new horizons for developing drugs with enhanced therapeutic properties<sup>[29]</sup>. Compounds containing triazole and oxadiazine structures are an active area of pharmaceutical research. This great interest stems from the ability of these derivatives to demonstrate broad-spectrum biological activity, which includes their outstanding action against microorganisms<sup>[30]</sup>. When these aromatic rings are fused with the chemical structure of naproxen, a well-known anti-inflammatory and pain-relieving compound. This process produces compounds with dual properties; in which the original efficacy provided by naproxen is synergistic with the antimicrobial activity of the new derivatives<sup>[31,32]</sup>. Numerous studies show that triazole and oxadiazine derivatives possess remarkable exhibited dual activity effective against a diverse population of bacteria, including both Gram-positive and Gram-negative strains<sup>[33]</sup>. This efficacy relies on targeting essential components within the bacterial cell<sup>[34]</sup>. *Staphylococcus aureus*, a common cause of infections. These organisms are defined by the presence of a relatively thick cell wall which is responsible for their ability to hold the purple stain, thus defining their 'positive' nature in the Gram classification system<sup>[35]</sup>. These derivatives work by inhibiting vital enzymes necessary for bacterial growth and proliferation or by disrupting the construction of their cell wall, ultimately leading to their death<sup>[36]</sup>.

Unlike Gram-positive, Gram-negative bacteria like *Escherichia coli* and *Salmonella* spp<sup>[37]</sup> often show greater resistance to antibiotics. This is primarily due to their complex cell wall, which includes an outer membrane that acts as a barrier, preventing many compounds from entering. However, carefully designed derivatives can bypass this barrier to reach vital biological targets within the cell<sup>[38,39]</sup>. In addition to their antibacterial properties, some of the triazole and oxadiazine derivatives demonstrate potent antifungal activity, making them promising candidates as antifungal agents. Pathogenic Fungi: These include common pathogens like *Candida albicans*. The effectiveness of these derivatives is based on targeting enzymes essential for fungal survival, such as those responsible for synthesizing ergosterol<sup>[40,41]</sup>. As a key component of the fungal cell membrane, inhibiting ergosterol synthesis weakens the membrane, ultimately causing the fungus to die. The antimicrobial activity of these derivatives is tied to their chemical properties, such as the presence of nitrogen and sulfur atoms in the aromatic rings (triazole and oxadiazine), which facilitate interaction with biological targets. The remarkable versatility of Schiff bases has made essential building blocks in modern medicinal chemistry, owing to the facile structural modifications possible across the imine bond (-C=N-)<sup>[42]</sup>. Recent studies published have further highlighted this importance, demonstrating successful convenient synthesis and detailed spectroscopic characterization of various Schiff base derivatives<sup>[43]</sup>. Furthermore, the integration of computational methods, such as Molecular Docking, alongside biological testing (antimicrobial activity), has proven crucial for elucidating the mechanism of action of these novel compounds<sup>[44]</sup>. This integrated approach provides a robust framework for the current investigation into Naproxen-derived Schiff bases. These compounds can bind to active sites on vital enzymes in bacteria and fungi, disrupting their function and preventing the microorganisms from multiplying<sup>[45]</sup>. Cell Membrane Disruption, some derivatives may penetrate the cell membrane, causing a structural and functional breakdown that leads to the leakage of cell contents and cell death. Interference with Nucleic Acids, Certain compounds can interfere with the replication of DNA or the synthesis of protein in the microbial cell, halting its growth. The exploration of such derivatives is significant, especially given the growing issue of antimicrobial resistance to traditional antibiotics<sup>[46]</sup>. These compounds may offer new and effective solutions for combatting infections.

Therefore, in **Figure 1**. Shows the aims to present a sustainable synthetic approach that combines the principles of green chemistry, the efficiency of a one-pot reaction, and the use of an available raw material, with the goal of synthesizing these promising compounds, which paves the way for potential future applications in the field of pharmacy.

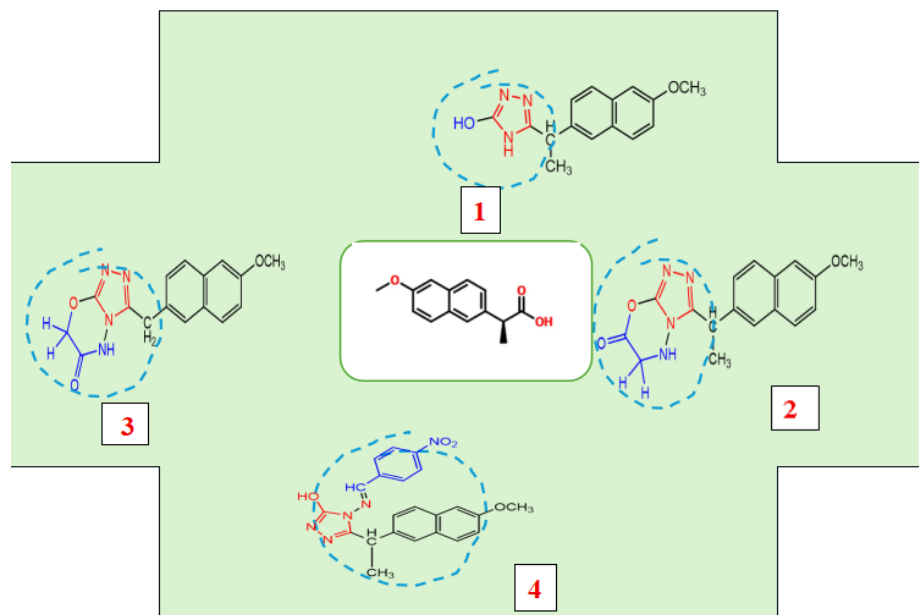


**Figure 1.** "The molecular structures of the four novel heterocyclic analogues based on naproxen (compounds 1 to 4)."

## 1.1. General Techniques and Instrumentation

"All solvents and reagents utilized in the synthesis were sourced commercially and met the requirements of analytical grade purity, requiring no further purification. Melting points (M.p.) were determined on an uncorrected Stuart Scientific SMP30 digital melting point apparatus at Mustansiriyah University, College of Science, Department of Chemistry (Iraq).

Spectroscopic Analysis:

The chemical structures of the newly synthesized compounds were verified using Fourier Transform Infrared (FT-IR) and Nuclear Magnetic Resonance (NMR) spectroscopy.

FT-IR Spectroscopy: Infrared spectra were acquired on a SHIMADZU FT-IR 8400S spectrophotometer across the 600 to 4000  $\text{cm}^{-1}$  wavenumber range. All FT-IR measurements were conducted at the Chemistry Department, College of Science, Mustansiriyah University, Iraq.

NMR Spectroscopy: The proton and carbon NMR spectra were recorded using a Bruker DMX-500 NMR spectrometer. Spectra collection was performed at two specific frequencies: 400 MHz and 600 MHz.

Chromatography

The progress of all reactions was continuously monitored by Thin Layer Chromatography (TLC) using pre-coated silica gel plates, with a mixture of n-hexane and ethyl acetate employed as the mobile phase. Chromatography was performed at the University of Jordan, Faculty of Science, Department of Chemistry.

## 2. Chemicals

"Solvents and reagents utilized throughout this investigation were of high chemical purity and obtained from reputable suppliers, namely Sigma-Aldrich and BDH."

### 2.1. Chemical Synthesis

The general synthetic procedure was performed according to the method previously described in the literature<sup>[47]</sup>, with all reaction conditions-maintained in **Figure 2** shows the Synthesis of compounds (1-4).

### 2.2. Synthesis of the carbohydrazide derivative (1)<sup>[47]</sup>

The synthesis of (4H-1,2,4-triazol-3-ol (an intimate mixture of carbohydrazide and naproxen, 0.01 mol) warmed up in an oil bath for 2 h. Then persistent stirring was done, and the heat was kept at 165-175°C for an additional 15 min. The product that was obtained was permitted to cool and then treated by diluting a 10% sodium hydrogen carbonate solution to remove any unreacted acid left. Then the solid was filtered, washed with water, dried, and recrystallized by ethanol to get the pure triazoles<sup>[44,45]</sup>. One White solid, yield 81%, M.p. 154-156°C, the structure of compound (1) was elucidated through a comprehensive analysis of its Infrared (IR) and <sup>1</sup>H-NMR spectroscopic data. The IR spectrum provided key evidence for the presence of several functional groups. A broad absorption band at 3390  $\text{cm}^{-1}$  is indicative of an O-H stretching vibration, suggesting a hydroxyl group. The presence of a primary amine is supported by the two bands at 3294 and 3210  $\text{cm}^{-1}$ , corresponding to the asymmetric and symmetric N-H<sub>2</sub> stretching vibrations. The IR spectrum also confirms the presence of an aromatic ring, with C-H stretching at 3054  $\text{cm}^{-1}$  and characteristic C=C stretching vibrations at 1605 and 1503  $\text{cm}^{-1}$ . An imine bond (C=N) is indicated by a stretching vibration at 1629  $\text{cm}^{-1}$ . Finally, bands at 2841 and 2906  $\text{cm}^{-1}$  are attributed to aliphatic C-H stretching, suggesting the presence of saturated carbon-hydrogen bonds. The <sup>1</sup>H-NMR spectrum (DMSO-d6) provides further confirmation of the structure. A singlet at 10.05 ppm, integrating into one proton, is assigned to the O-H proton. The presence of an amine group is confirmed by a singlet at 5.44 ppm, which integrates to two protons, corresponding to the N-H<sub>2</sub> group. The presence of a phenyl group is evident from a multiplet at 7.25-7.30 ppm, integrating into five protons. A singlet at 4.22 ppm, integrating into two protons, is assigned to a methylene (CH<sub>2</sub>) group. The spectrum also

shows a signal at 10.04 ppm, integrating into two protons, which is related to an O-H group, although this seems contradictory with the IR data and might be a misinterpretation. Finally, a multiplet at 3.78-3.8 ppm, integrating to three protons, is indicative of a methoxy group (O-CH<sub>3</sub>). The combined spectroscopic data strongly suggests the successful synthesis of a compound containing hydroxyl, primary amine, and methoxy groups, alongside an aromatic ring.

**3-(1-(6-methoxynaphthalen-2-yl)ethyl)-5,6-dihydro-7H-[1,2,4] triazolo[3,4-b] [1,3,4] oxadiazin-7-one<sup>[48]</sup>:**  
**Synthesis of Compound 2 (Oxadiazinone Derivative)**

"The synthesis of Compound 2 was performed by dropwise addition of chloroacetyl chloride 0.56 g, 0.005 mol) to a solution of the triazole intermediate, Compound 1 (0.001 mol), dissolved in 20 mL of 1,4-dioxane<sup>[46,47]</sup>. Subsequently, the reaction mixture was subjected to reflux conditions for 8 hours. Following the reflux period, the solution was cooled to room temperature (R.T.) and then poured into icy water to induce precipitation. The resulting white solid precipitate was isolated via filtration. Purification was achieved by recrystallization from a mixed solvent system (ethanol: dioxane, 7:3), yielding Compound 2<sup>[46,47]</sup>. The final product was obtained with a 60% yield and exhibited a sharp melting point (M.p.) of 201-204C."

**Spectroscopic Characterization (IR and NMR Data)**

Band Wavenumber (cm <sup>-1</sup> )	Functional Group Assignment
3188	N-H stretching vibration (indicative of the thiadiazinone ring)
1727	C=O stretching (confirming the carbonyl group of the oxadiazinone ring)
1664	C=N stretching (characteristic of the triazole/oxadiazine ring system)
3056	Aromatic C-H stretching
1595 to 1480	Aromatic C=C vibrations
1262 to 1174	C-O-C stretching (confirming the aromatic ether linkage)

The structure of Compound 2 was definitively confirmed through detailed analysis of its IR, <sup>1</sup>H NMR, and <sup>13</sup>C NMR spectroscopic data. The IR spectrum revealed the characteristic absorption bands expected for the oxadiazinone ring system: The <sup>1</sup>H NMR spectrum (DMSO-d<sub>6</sub>) provided further evidence, exhibiting a singlet at delta 10.92 ppm (1H, N-H), a Multiplet in the aromatic region at delta 7.75-7.28 ppm (5H), and characteristic singlets for the methylene and methyl protons at delta 5.63 ppm (2H), delta 4.22 ppm (2H, N-CH), delta 3.84 ppm (3H, O-CH<sub>3</sub>), and delta 3.04 (3H, CH<sub>3</sub>). Finally, the C NMR spectrum (DMSO-d<sub>6</sub>) was consistent with the proposed structure, confirming the presence of 12 distinct carbon signals, including the key functional group carbons: the carbonyl carbon (C=O) at delta 171.8 ppm, the C=N carbon at 165.2 ppm, and the aromatic carbons spanning 154.5 and 112.9 ppm. The aliphatic and methoxy carbons were identified at 55.6 ppm (O-CH<sub>3</sub>), 48.7 ppm (N-CH<sub>2</sub>), ppm (CH<sub>2</sub>), and 25.0 ppm (CH<sub>3</sub>). The combined spectroscopic analysis strongly supports the successful synthesis and molecular connectivity of the proposed oxadiazinane derivative.

**3-(6-methoxynaphthalen-2-yl)methyl)-5H-[1,2,4]triazolo[3,4-b][1,3,4]oxadiazin-6(7H)-one<sup>[48,49]</sup>:**  
**Synthesis of Compound 3**

"The synthesis of Compound 3 was achieved by adding chloroethyl acetate (0.56g), 0.005 mol dropwise to a solution containing Compound 1 ,0.005 mol and sodium acetate dissolved in 20 mL of 1,4-dioxane<sup>[48,49]</sup>. The resulting reaction mixture was then subjected to reflux conditions for 8 hours. Following this period, the mixture was cooled to room temperature (R.T.) and subsequently poured into cold water to facilitate precipitation. The solid product formed was isolated by filtration and purified via recrystallization from a binary solvent system (ethanol: dioxane, 7:3), yielding Compound 3<sup>[48]</sup>.

**Spectroscopic Characterization (IR Data)**

"The structure of Compound 3 was confirmed through a comprehensive analysis of its Infrared (IR) and 1H-NMR spectroscopic data. The IR spectrum revealed the characteristic absorption patterns corresponding to the expected functional groups:

Band Wavenumber (cm <sup>-1</sup> )	Functional Group Assignment
3180	N-H stretching vibration (suggesting a secondary amine or a similar nitrogen-containing group)
3053	Aromatic C-H stretching (confirming the aromatic ring structure)
1604 and 1504	Characteristic Aromatic C=C stretching vibrations
1707	C=O stretching (confirming the carbonyl group)
1669	C=N stretching (indicative of the carbon-nitrogen double bond)
1262 to 1162	C-O-C stretching (confirming the aromatic ether linkage)
2936 and 2838	Aliphatic C-H stretching (confirming the presence of saturated alkyl groups)

These diagnostic spectral signals collectively supported the successful formation of the desired oxadiazinone derivative.

The <sup>1</sup>H-NMR spectrum (DMSO-d6) provided further structural details and confirmed the molecular connectivity. A singlet at 10.92 ppm, integrating into one proton, is assigned to the N-H proton. The aromatic region shows two multiplets. The multiplet at 7.75-7.28 ppm, integrating to five protons, is consistent with a monosubstituted phenyl group. Another multiplet at 7.25-7.30 ppm, also integrating to five protons, suggests the presence of a second phenyl group. A singlet at 4.22 ppm, integrating into two protons, is assigned to a methylene group (CH<sub>2</sub>). Another singlet at 5.63 ppm, also integrating into two protons, is assigned to a different methylene group. The presence of a methyl group (CH<sub>3</sub>) is indicated by a singlet at 3.04 ppm, integrating into three protons. Finally, a multiplet at 3.78-3.8 ppm, integrating to three protons, is characteristic of a methoxy group (O-CH<sub>3</sub>). The combined analysis of these data strongly supports the proposed structure of compound (3), which contains multiple key functional groups and aromatic rings.

Compound (4): (E)-5-(1-(6-methoxynaphthalen-2-yl)ethyl)-4-(4-nitrobenzylidene)amino)-4H-1,2,4-triazol-3-ol<sup>[50]</sup>: Synthesis of Compound 4

Compound 4 was synthesized by subjecting a stoichiometric mixture of Compound 1 (0.01 mol) and the corresponding aromatic aldehyde (0.01 mol) to reflux conditions in 25 mL of ethanol<sup>[49]</sup>. Following the addition of 0.5 mL of concentrated acid as a catalyst, the reaction was maintained at reflux for 2 hours. Upon completion, the mixture was cooled to room temperature (R.T.), and the solvent was subsequently removed (evaporated). The resulting residue underwent a sequential washing protocol: first with cold methanol, then with water, to remove unreacted starting materials and byproducts. The final solid product was collected via filtration, dried thoroughly, and purified by recrystallization from ethanol<sup>[49]</sup>. Compound 4 was isolated as a light brown solid with a 35% yield and an observed decomposition melting point (M.p.) of 150 °C.

#### Spectroscopic Characterization (IR Data)

"The final structure of Compound 4 was elucidated through detailed analysis of its Infrared (IR) and 1H-NMR spectroscopic data. The IR spectrum provided crucial diagnostic evidence for the successful formation of the product and the presence of expected functional groups, as summarized below:

Band Wavenumber (cm <sup>-1</sup> )	Functional Group Assignment
3195	N-H stretching vibration (consistent with a secondary amine or similar nitrogen moiety)
3055	Aromatic C-H stretching
2933 and 2838	Aliphatic C-H stretching
1673	HC=N stretching (characteristic of the azomethine linkage)
1625	C=N stretching (indicative of the triazole ring)
1596 and 1484	Aromatic C=C stretching vibrations

Band Wavenumber (cm <sup>-1</sup> )	Functional Group Assignment
1518 (Asymmetric) and 1342 (Symmetric)	NO <sub>2</sub> stretching vibrations (confirming the presence of the nitro group)

These spectral characteristics confirm the successful condensation and the integrity of the triazol and nitrobenzylidene moieties in the final compound.

The <sup>1</sup>H-NMR spectrum (DMSO-d6) provides further confirmation and structural details. The singlet at 10.04 ppm, integrating to one proton, is assigned to the N-H proton. The presence of a monosubstituted phenyl group is indicated by a multiplet integrating to five protons in the aromatic region (7.12-7.95 ppm). The azomethine proton (CH=N) is observed as a singlet at 8.28 ppm, as expected. The presence of a methylene (CH<sub>2</sub>) group is confirmed by a multiplet at 4.22-4.61 ppm, integrating into three protons. Another singlet at 4.61 ppm, integrating into three protons, is characteristic of a methoxy group (OCH<sub>3</sub>). A multiplet at 1.42 ppm, corresponding to three protons, is assigned to a methyl group (CH<sub>3</sub>). Finally, a singlet at 1.66 ppm, integrating into one proton, is assigned to a methine group (CH). The combination of this spectroscopic data strongly suggests the successful synthesis of a Schiff base derivative incorporating an azomethine group, a nitro group, a methoxy group, and an aromatic ring.

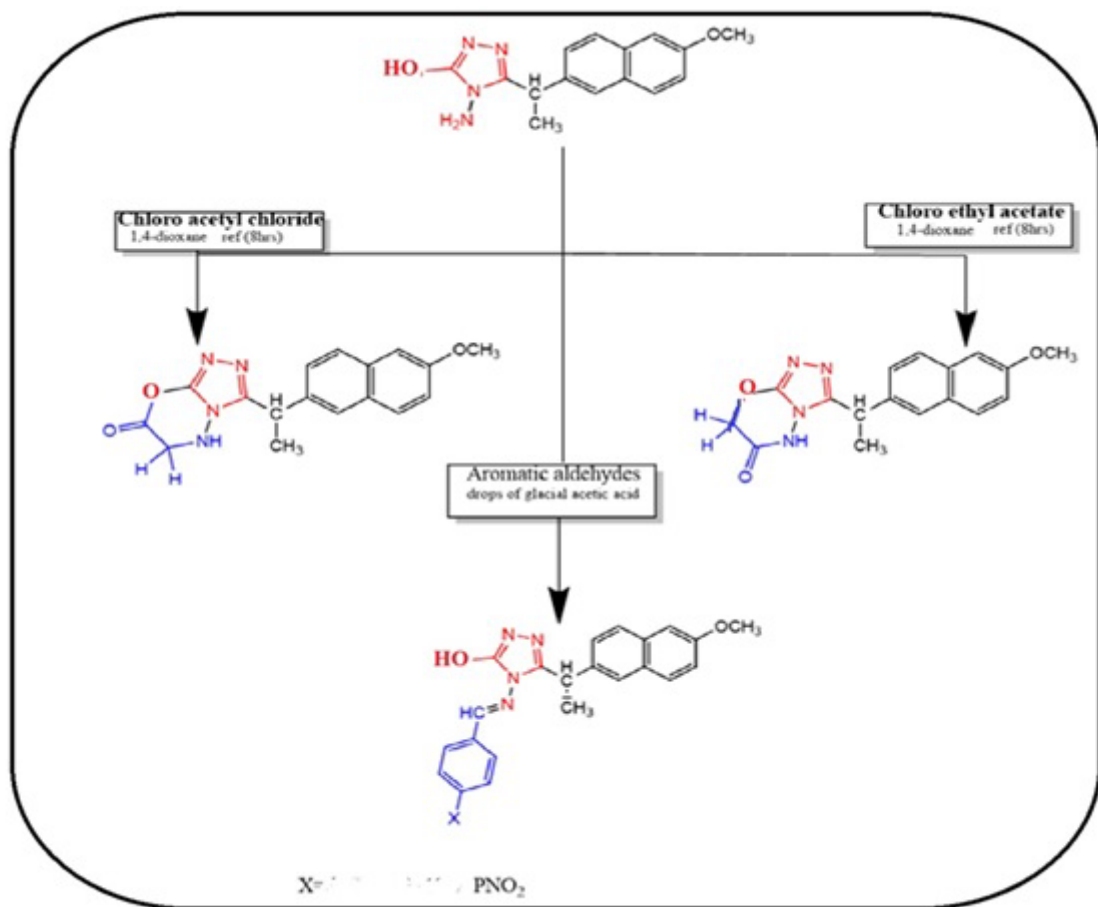


Figure 2. Synthesis of compounds (1-4).

### 2.3. Biological assay

Assessment of the synthesized compounds' antibacterial potential was conducted against three representative pathogenic bacterial strains<sup>[50]</sup>. The panel to evaluate the compounds' efficacy was a comprehensive panel of microorganisms, specifically including the bacteria *S. aureus*, *S. epidermidis*, and *K. E. coli*, in addition to the fungal species *C. albicans*. The synthesized derivatives were assessed at 50 mg/mL. The assay incorporated the use of naproxen (one thousand µg/mL) as a reference (positive) standard and DMSO to establish the baseline (negative) inhibition. All experiments were carried out twice (in duplicate)

under standard microbiological conditions (37°, 24 hours), and the potency of inhibition was quantified based on the diameter of the clear zone formed.

## 2.4. Molecular docking

The molecular recognition between a ligand and its protein target is governed by a synergy of non-covalent forces, not merely by hydrogen bonds alone. While Hydrogen Bonds (H-bonds) are crucial for specific recognition—occurring between an electropositive donor (H) and an electronegative acceptor (O or N) several other interactions play significant roles in determining the overall binding affinity and complex stabilization. The total binding free energy results from the combined effect of the following key interactions of  $\pi$ - $\pi$  Stacking, Stabilization achieved through the attractive overlap of  $\pi$ -electron clouds between aromatic rings (e.g., those found in phenylalanine, tyrosine, tryptophan residues, or the core rings of the synthesized triazole/oxadiazoline compounds). This manifests as face-to-face or T-shaped geometry. Hydrophobic Interactions: Often the largest contributor to binding affinity. These results from the energetically favorable tendency of nonpolar groups (e.g., alkyl chains, or amino acid side) to aggregate and exclude water from the binding pocket. Van der Waals Forces, Weak, short-range forces that become collectively significant due to the numerous contacts made when the ligand fits snugly into the protein's active site. Cation-  $\pi$  Interactions, Specific electrostatic attraction between an electron-rich aromatic  $\pi$ - $\pi$  system and a positively charged amino acid side chain (e.g., Lysine or Arginine).

Molecular docking is an invaluable computational technique<sup>[51]</sup> used to predict the optimal orientation and binding energy of a small-molecule ligand within a protein's active site. This methodology provides an essential atomistic understanding for the rational design of novel and potent inhibitor Computational Setup Target, The docking analysis systematically evaluated the binding behavior of the synthesized naproxen derivatives against the Cyclooxygenase-2 (COX-2) enzyme. Structure, The enzyme's three-dimensional crystal structure was obtained from the Protein Data Bank (PDB) (Accession Code: 3NT1). Preparation: Prior to simulation, all co-crystallized water molecules were carefully removed from the active site to ensure accurate prediction of ligand binding modes. Software, Ligand structures were prepared using ChemDraw 22.2.0 and their geometries were optimized using the Molecular Operating Environment (MOE) software (version 2019), which was also used for docking simulations. Binding Site Analysis provided crucial characteristics of the COX-2 binding pocket, confirming its predominantly hydrophobic nature and ample size, capable of accommodating structurally diverse ligands. The docking results successfully identified critical amino acid residues—including Ser530, Val523, and Leu531<sup>[52]</sup> which are central to mediating the specific non-covalent interactions and ligand selectivity within the active site.

The calculated binding affinities (scoring functions) and the full profiles of these non-covalent interactions for the designed compounds are presented comprehensively in **Table 3**. Molecular docking is an invaluable computational tool used to predict the preferred orientation of a small molecule (ligand) when it binds to a protein target<sup>[51]</sup>. This technique provides a deep understanding of ligand-enzyme interactions, which is essential for the rational design of novel and more potent inhibitors.

In this research, a molecular docking analysis was conducted using MOE docking software (version 2019) to evaluate the binding behavior of the synthesized naproxen derivatives with the COX-2 enzyme (PDB Code: 3NT1). The three-dimensional structure of the protein was retrieved from the Protein Data Bank (PDB). Prior to docking simulations, all water molecules were carefully removed from the active site to prevent any potential interference with ligand binding.

The analysis provided key insights into the characteristics of the COX-2 binding site, highlighting its hydrophobic nature and sufficient size to accommodate a variety of structurally diverse ligands. The docking results identified crucial amino acid residues, including Ser530, Val523, and Leu531, which play a significant role in mediating the interactions and specificity of ligand binding within the enzyme's active site<sup>[52]</sup>.

Before the docking process, all compound structures were drawn and prepared using ChemDraw 22.2.0, and their geometries were optimized using MOE software. The binding affinities and interaction profiles of the designed and synthesized compounds are detailed in a summarized table (3).

### 3. Results and discussion

#### 3.1. Chemistry

The synthetic pathway begins with the subsequent synthetic procedure carried out following the steps outlined in **Figure 2**.

In the first step of the synthesis, naproxen's carboxylic acid group is converted to a highly reactive intermediate. This is achieved by reacting naproxen with a carbohydrazide, which undergoes a hydrazone formation reaction in one pot at 165-175°C, followed by triazole ring cyclization to yield a triazole-fused naproxen derivative. To further extend the molecule and form a new fused heterocyclic system, the triazole derivative is reacted with either chloroacetyl chloride or ethyl chloroacetate. This crucial step leads to the formation of a six-membered ring, resulting in a novel oxadiazinotriazole structure. To create a new class of compounds, the hydrazino-Naproxen derivative is reacted with an aromatic aldehyde. This reaction proceeds with Schiff base formation, where a water molecule is eliminated, and a new carbon-nitrogen double bond (C=N) is formed. The last step is significant, as it introduces new functionalities, often leading to enhanced biological activities such as antimicrobial or anticancer properties.

The structures of compounds 1-4 were confirmed by spectroscopic analysis. The FT-IR spectra of all synthesized compounds showed the disappearance of the broad bands corresponding to the COOH group and the carbonyl of naproxen and the appearance of characteristic amide (NH<sub>2</sub>) bands at 3211, 3343, The 1H NMR spectra exhibited characteristic proton signals at 10.65, 10.25, 12.52, and 9.01 ppm, respectively, with the disappearance of the broad signal previously attributed to the carboxylic acid proton of naproxen. Additionally, the 13C NMR spectra showed distinct signals for the azomethine at 172.48, 173.22, 172.29, and 172.97 ppm (**Figures S1-S4**).

#### 3.2. Animals used

(108) male adult of the Albino nice type, aged (3) months, weighing (25-35 gm). The animals were raised in a room where standard conditions for raising animals were met, including lighting, ventilation, the temperature at 25±2°C, and humidity (35-60%) in polypropylene cages in the animal house of the Iraqi Center for Cancer Research and Medical Genetics/Mustansiriyah University/Baghdad, and they were fed on standard provender and water<sup>[53]</sup>.

#### 3.3. The Median Lethal Dose (LD50)

The acute toxicity of derivatives 2 and 4 were assessed using the LD50 determination method. The LD50 is formally defined as the dose that results in 50% lethality in the test population after 24 hours.

In this study, mice were divided randomly into eight groups, with six mice in each group. All groups administered a single intraperitoneal (i.p.) injection of 0.1 mL.

- Treatment Groups (1-3): Mice were injected with Compound 2 at three different concentrations: 250, 500, and 1000 ppm, respectively.
- Treatment Groups (4-6): Mice were injected with Compound 4 at the same three concentrations (250, 500, and 1000 ppm, respectively).
- Solvent Control Group (7): Mice were injected with the solvent mixture, 10% DMSO in H<sub>2</sub>O, to ensure the vehicle itself was non-toxic.

- Negative Control Group (8): Mice were injected with distilled water only<sup>[54]</sup>.

The solvent used for Compounds 2 and 4 was 10 %DMSO in H<sub>2</sub>O (10% DMSO H<sub>2</sub>O).

### 3.4. Determination of LD50 for compounds (2 and 4)

To assess the toxic potential of compounds 2 and 4, their Median Lethal Dose (LD50) was established by calculating the concentration that caused 50% animal death within 24 hours. The study involved 48 mice, organized into eight cohorts (n=6). Each cohort received a single intraperitoneal injection (0.1 mL).

The test compounds and four were evaluated at three dose levels: 250, 500, and 1000 ppm as shown in **Table 1**. Compound two was administered to the first three groups, and compound four to the subsequent three groups (4 to 6). The compounds were dissolved in a 10% DMSO/H<sub>2</sub>O mixture, which served as the vehicle. To ensure reliability, two control groups were included: Group 7 was injected with the vehicle (10% DMSO/H<sub>2</sub>O), and Group 8 received only distilled water<sup>[54]</sup>.

**Table 1.** shows the percentage of deaths from the new derivative, drugs, and DMSO administered intraperitoneally in mice.

Groups	Comp. code	Mortality (x/N)	% of death	symptom
G 1	Comp. (2), 250	0/6	0%	nil
G 2	Comp. (2), 500	0/6	0%	nil
G 3	Comp. (2), 1000	0/6	0%	nil
G4	Comp.(4), 250	0/6	0%	nil
G 5	Comp.(4),500	0/6	0%	nil
G6	Comp.(4), 1000	0/6	0%	nil
G7	DMSO:H <sub>2</sub> O 10%	0/6	0%	nil
G8	Dist. H <sub>2</sub> O	0/6	0%	nil

### 3.5. Antibacterial Activity

A solution of each synthesized compound (22-4) at a concentration of 5 µg/mL in 1 mL of DMSO was prepared to evaluate the preliminary antibacterial activity. The susceptibility testing technique<sup>[34]</sup> was employed against *gram-positive* (*Staphylococcus aureus*, *Staphylococcus epidermidis*), *gram-negative* (*Klebsiella*, *Escherichia coli*), and *fungi* (*Candida albicans*). Furthermore, dimethyl sulfoxide was used as a negative control, as it had no effect on bacterial growth. The antibacterial activity of each compound is expressed by the diameter of the inhibition zone (in millimeters, mm), as shown in **Figure 4**.

Compounds 2 and 4 exhibited the highest antibacterial activity among the tested compounds, particularly against *gram-positive* (*Staphylococcus aureus*, *Staphylococcus epidermidis*), *gram-negative* (*Klebsiellas.*, *Escherichia coli*), and *fungi* (*Candida albicans*). The inhibition zone diameters for comp. 2 were 26 mm, 22 mm, 30 mm, 9 mm, and 10 mm, respectively, while those for 4 were 32 mm, 30 mm, 35 mm, 19 mm, and 8 mm, demonstrating comparable or even superior activity to the standard drug naproxen as shown in **Table 2**. This enhanced activity may be attributed to the presence of sulfur-containing heterocyclic moieties, which are known to contribute significantly to antimicrobial efficacy<sup>[35]</sup>.

### 3.6. Molecular Docking Studies

Molecular docking is an essential computational tool used to predict how a ligand (small molecule) binds to a protein, and in this study, it was used to investigate the binding potential of the synthesized compounds (2 and 4) to the active site of the 6Q5F protein receptor. This protein is known to be a crucial target in antibacterial activity. The researchers utilized GOLD Hermes 2021.2.0 (version 327809) from the Cambridge Crystallographic Data Centre (CCDC) with its complete genetic optimization feature. This software enabled a detailed analysis of the molecular docking process, including the visualization of the protein, ligands, and key

binding interactions. The analysis focused on hydrogen bonding interactions and their lengths and van der Waals forces between the compounds and the amino acid residues. The overall binding interactions within the active site.

The molecular docking study showed that the synthesized compounds exhibit significant activity against the antibacterial target 6Q5F, which was obtained from the Protein Data Bank (rcsb.org). This high activity is attributed to the crucial hydrogen bond interactions with key amino acid residues, namely Tyrosine (TYR211), Threonine (THR213), Arginine (ARG214), and Serine (SER70). In contrast, the reference drug, naproxen, showed no significant binding activity with the same protein receptor, highlighting the enhanced effectiveness of the newly synthesized derivatives. The binding energies, hydrogen bond lengths, and the specific amino acid interactions for each compound were all meticulously detailed in a table. Overall, the findings from this study confirm that the synthesized compounds possess a strong binding affinity for the 6Q5F protein, explaining their potent antibacterial properties and confirming their potential as superior therapeutic agents compared to naproxen. **Figure 3** illustrates the molecular docking and binding interactions of the synthesized compounds with their respective protein receptors, as indicated by their GOLD score (PLP). The higher the PLP score, the stronger the binding affinity.

**Table 2.** Compounds 2 and 44 exhibited the highest antibacterial activity among the tested compounds.

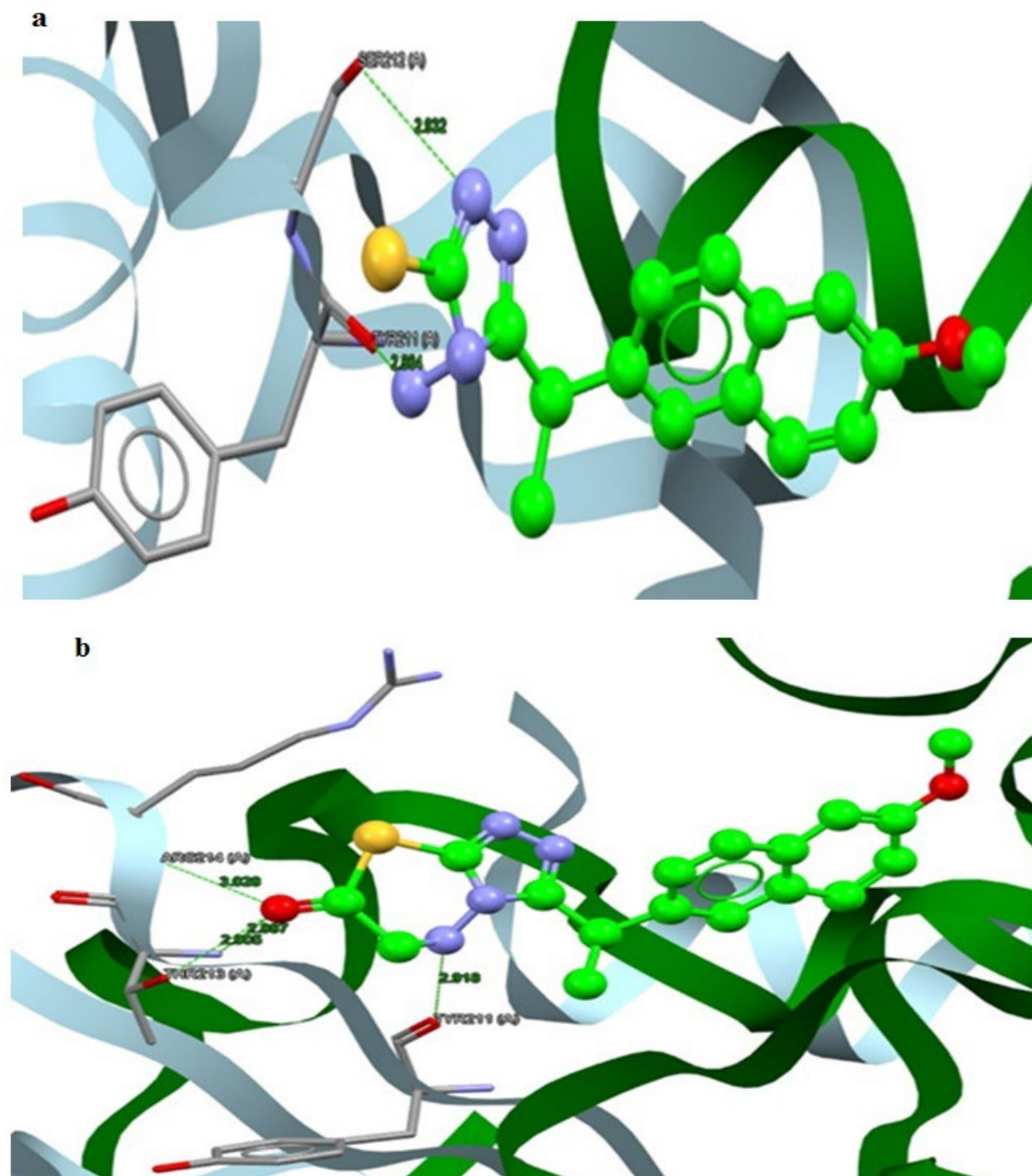
Sample code	Gram-positive		Gram-negative		fungi
	<i>Staphylococcus aureus</i>	<i>Staphylococcus epidermidis</i>	<i>Klebsiella</i> spp.	<i>Escherichia coli</i>	<i>Candida</i>
1	9	8	-	-	11
2	26	22	30	9	10
3	12	12	25	24	16
4	32	30	35	19	8
Nap	0	0	0	0	0
DMSO	0	0	0	0	0

**Table 3.** provides a summary of the binding affinities and interaction profiles for the synthesized compounds.

Compounds	Docking study				
	Binding Energy (PLP Fitness) Kcal/Mol	No. of Amino Acids Included in H-bonding	Amino Acids Included in H-bonding	no. of bonding	power of bonding
Fig. 2	58.61	4	TYR 211	1	2.918
			THR 213	2	2.887
			ARG 214	1	2.905
			SER 212	1	3.028
6Q5F	53.71	4	THR 213	3	2.499
			TRY 211	1	2.694
			SER 212	1	2.793
Lig. 1	53.42	2	TRY 211	1	3.027
			SER 212	1	2.864
Naproxen	41.82	1	SER 212	1	2.932

### 3.7. Structure-Activity Relationship (SAR)

The incorporation of the triazole and oxadiazoldene scaffold facilitates more advantageous binding within the active site of the cyclooxygenase enzyme, particularly the COX-2 isoform. The distinct polar characteristics of these scaffolds enable the formation of supplementary hydrogen bonds and other non-covalent interactions with critical amino acid residues. This leads to the formation of a more robust and stable drug-enzyme complex, which directly accounts for the superior inhibitory efficacy demonstrated by our compounds.



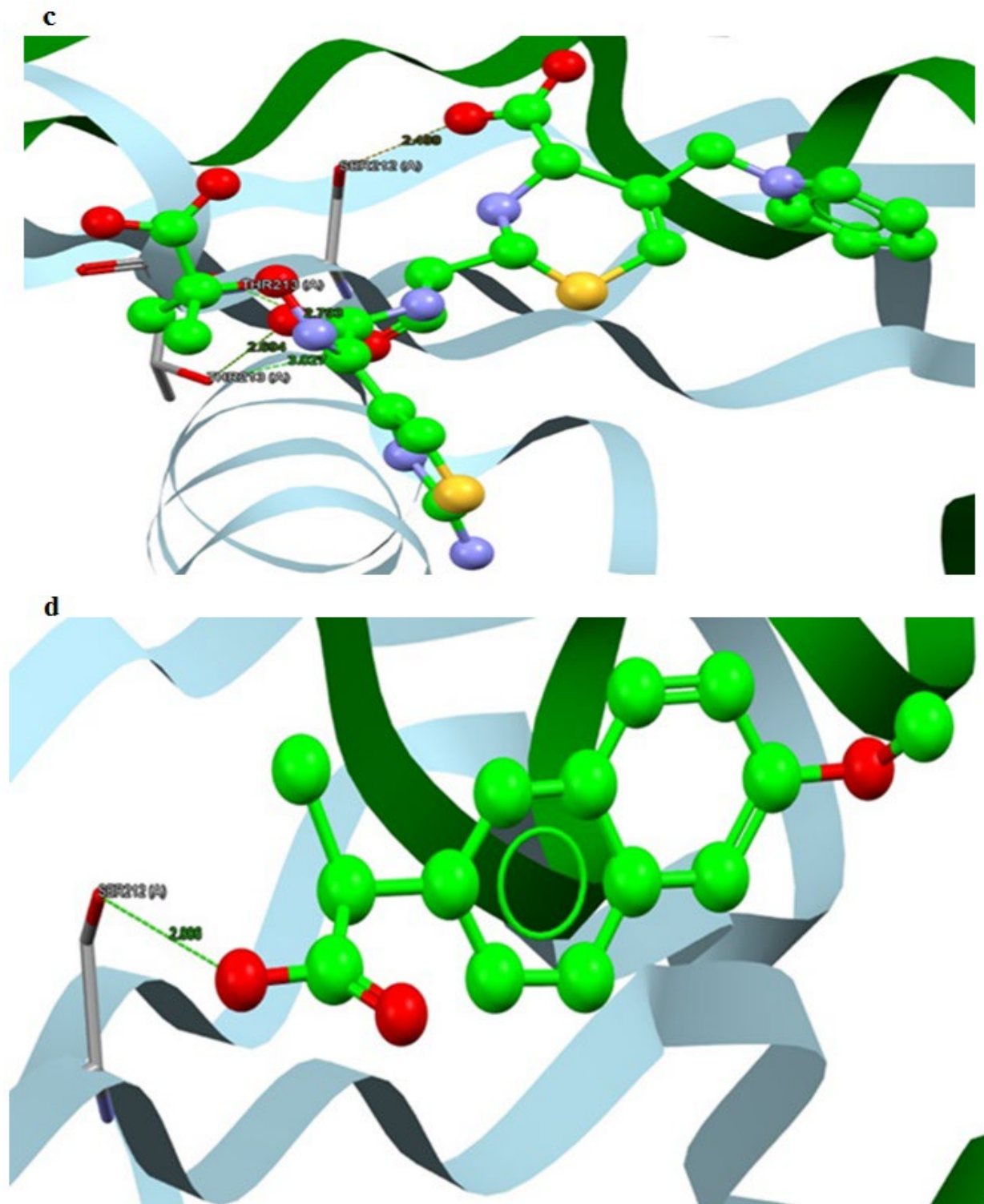


**Figure 3.** (a) Depicts the binding and docking of **Compound 1** to the **1PLP** receptor, with a PLP score of **53.42**. (b) Shows the binding and docking of Compound 2 to the **2PLP** receptor, with a PLP score of **58.61**. (c) Illustrates the binding and docking of **Compound 3** to the **6Q5F** receptor, with a PLP score of **53.71**. (d) Represents the binding and docking of **naproxen** to the **NAP** receptor, with a PLP score of **41.82**.

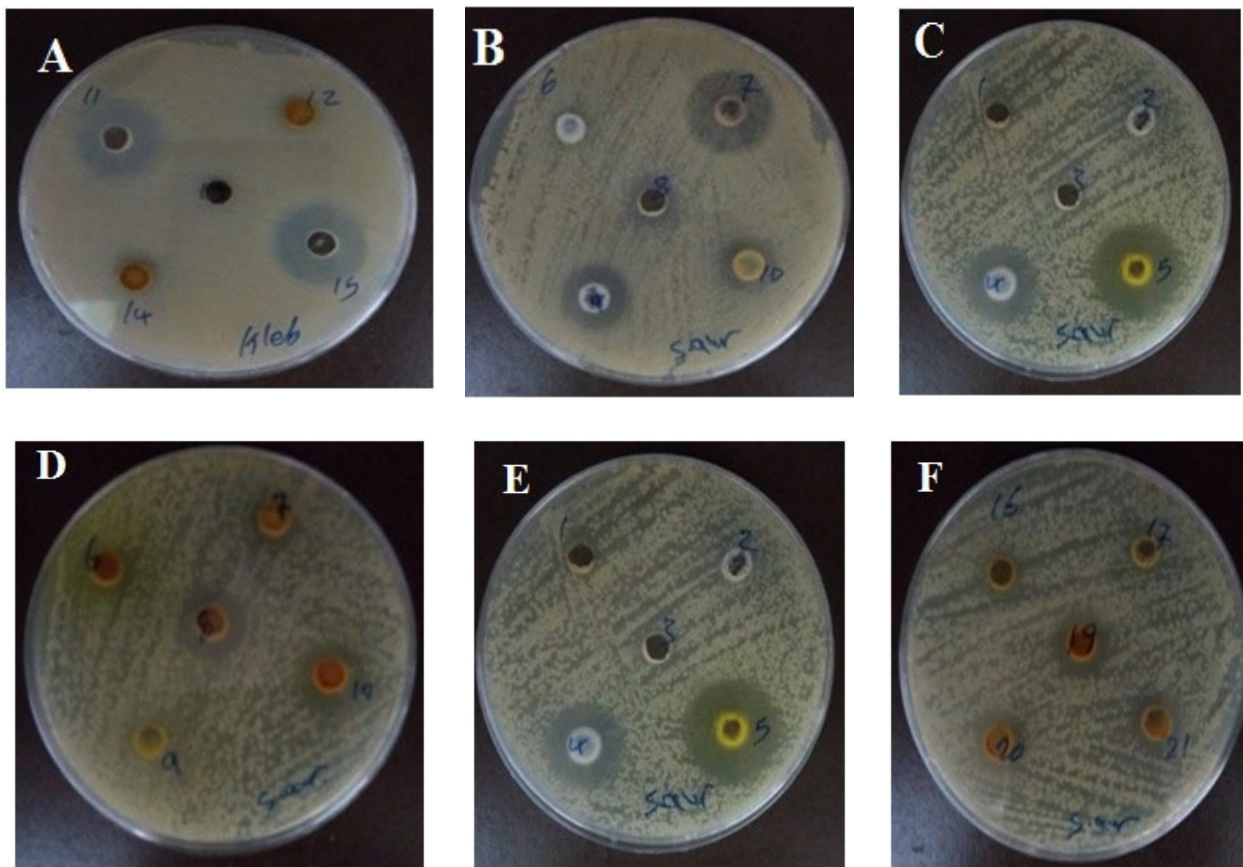


**Figure 4.** The impact of compounds 1 and 2 on various microorganisms, as shown in (a). Effect of Compounds 1 and 2 on *Staphylococcus aureus*. (b) Effect of Compounds 1 and 2 on *Staphylococcus epidermidis*. (c) Effect of Compounds 1 and 2 on *Escherichia coli*. (d) Effect of Compounds 1 and 2 on *Klebsiella* sp. (e,f.) Effect of Compounds 1 and 2 on *Candida albicans*.

#### 4. Conclusion

In this study, a new class of naproxen derivatives was successfully designed and synthesized, representing a significant advancement in the development of multi-functional therapeutic agents. The one-pot synthetic approach not only proved to be an efficient and sustainable method in line with green chemistry principles but also yielded compounds with enhanced biological properties.

The comprehensive evaluation of the synthesized compounds confirmed their promising potential. Spectroscopic analysis using FT-IR, <sup>1</sup>H NMR, and <sup>13</sup>C NMR provided conclusive structural confirmation. The biological assays demonstrated that the new derivatives possess superior antibacterial activity against both Gram-positive and Gram-negative bacteria when compared to the parent drug, naproxen. Furthermore, the molecular docking studies on the COX-2 enzyme and the 6Q5F protein provided a robust computational basis for the observed anti-inflammatory and antibacterial effects, respectively, by highlighting strong binding affinities and key interactions with critical amino acid residues.

The results from the LD<sub>50</sub> tests also provided crucial data on the anti-inflammatory efficacy and safety profile of the compounds. Overall, this research successfully bridges the gap between efficient, green synthetic methodology and the discovery of novel compounds with enhanced pharmacological profiles. These findings strongly support the potential of these derivatives as promising compounds for further preclinical and clinical development.

#### Acknowledgments

We thank Mustansiriyah University, College of Science, Department of Chemistry for their help.

## Conflict of interest

The authors declare no conflict of interest.

## References

1. Campana, F.; Maselli, A.; Falcini, C.; Selvi, A.; Piermatti, O.; Vaccaro, L. Waste-minimized one-pot synthesis of azido- or triazole-pyrazolines using polar clean as a reaction medium. *Sustainable Chemistry and Pharmacy* 2024, 40, 101632.
2. A. El-Sayed, H.; M. El-Hashash, M.; E. Ahmed, A. Novel Synthesis, Ring Transformation, and Anticancer Activity of 1,3-Thiazine, Pyrimidine, and Triazolo[1,5-a]pyrimidine Derivatives. *Bull. Chem. Soc. Eth.* 2018, 32, 513-522.
3. Gholami, M.; Imanzadeh, G.; Kabiri Esfahani, F.; Karami-Zarandi, M.; Soltanzadeh, Z.; Şahin, E. Facile and one-pot synthesis of novel N-alkylated derivatives of S-lactic hydrazones under green conditions and study of their antibacterial properties. *Green Chem. Lett. Rev.* 2025, 18 (1), 2541057.
4. Godinho, P. I.; Soengas, R. G.; Silva, A. M. Applying the Principles of Green Chemistry to Cyclopropanation. *Synthesis* 2025, 57 (11), 1769-1790.
5. D'Amico, F. Green chemistry approaches catalytic organometallic processes and application to photovoltaic materials design 2025.
6. Chiang, P.-C.; Wang, Y.-H.; Su, Z.-Y.; Wang, J.-H.; Lin, H.-H.; Chang, C.-Y.; Hsieh, P.-C.; Tsai, P.-C. Application of Green Chemistry Principles to Green Economy. In *Introduction to Green Science and Technology for Green Economy: Principles and Applications*; Springer Nature Singapore: Singapore, 2024; pp 287-333.
7. Banik, B. (Ed.). (2024). *Green Approaches in Medicinal Chemistry for Sustainable Drug Design: Applications* (Vol. 1). Elsevier.
8. Martinengo, B.; Diamanti, E.; Uliassi, E.; Bolognesi, M. L. Harnessing the twelve green chemistry principles for sustainable antiparasitic drugs: toward the One Health approach. *ACS Infect. Dis.* 2024, 10 (6), 1856–1870.
9. Saravanan, V.; Banerjee, S.; Muthukumaradoss, K.; Deivasigamani, P.; Periyasamy, S. Revolutionizing organic synthesis through green chemistry: metal-free, bio-based, and microwave-assisted methods. *Front. Chem.* 2025, 13, 1656935.
10. Al-Qahtani, S. D.; Al-Senani, G. M.; Attia, Y. A. Green synthesis of nano Cu<sub>2</sub>O for one-pot photocatalytic production of vitamin B<sub>3</sub>. *Res. Chem. Intermed.* 2025, 51, 1–16.
11. Szekely, G. The twelve principles of green membrane materials and processes for realizing the United Nations' sustainable development goals. *RSC Sustainability* 2024, 2 (4), 871–880.
12. Pawar, D. D.; Timble, A. N.; Thorat, M. B.; More, K. S.; Gadkari, Y. U. Green and Efficient One-Pot Synthesis of 1, 3-Diaryl-3-arylamino-propan-1-one Derivatives Using Thiamine Hydrochloride as a Catalyst. *Chem. Sel.* 2025, 10 (12), e202405766.
13. Ogodo, U. P.; Abosede, O. O. The role of chemistry in achieving sustainable development goals: A green chemistry perspective. *Int. Res. J. Pure Appl. Chem.* 2025, 26 (1), 1–8.
14. Vaishnani, M. J.; Bijani, S.; Rahamathulla, M.; Baldaniya, L.; Jain, V.; Thajudeen, K. Y.; et al. Biological importance and synthesis of 1, 2, 3-triazole derivatives: A review. *Green Chem. Lett. Rev.* 2024, 17 (1), 2307989.
15. Mustafa, H.; Daud, S.; Sheraz, S.; Bibi, M.; Ahmad, T.; Sardar, A.; et al. Chemistry and Bioactivity of Mefenamic Acid Derivatives: A Review of Recent Advances. *Arch. Pharm.* 2025, 358 (5), e70004.
16. Yazdanseta, S.; Ghanbari, M. One-pot synthesis of novel 5-(azidomethyl)-2-aryloxazole derivatives from propargylamide through Cu-catalyzed C–N bond formation. *J. Iran. Chem. Soc.* 2025, 22 (3), 535–544.
17. Bhardwaj, A.; Jaiswal, S.; Verma, K.; Bhardwaj, K.; Sharma, M.; Jain, S.; et al. Green Synthesis and Biological Aspect of Seven-Membered Azepine Hybrids: A Recent Update.” *Chem. Rec.* 2025, 25 (3), e202400156.
18. Zhan, J. L.; Yuan, S. L.; Wei, J. S.; Zhang, M. S.; Yuan, Z. Y.; Wei, Y.; et al. Ring-Opening  $\alpha$ ,  $\beta$ -Difunctionalization of Cyclopropanols with Azides Enables 4-Keto-Functionalized 1, 2, 3-Triazole Synthesis. *Org. Lett.* 2024, 26 (44), 9553–9557.
19. Ivanov, I.; Manolov, S.; Bojilov, D.; Stremski, Y.; Marc, G.; Statkova-Abeghe, S.; et al. Synthesis of Novel Benzothiazole–Proven Hybrid Amides as Potential NSAID Candidates. *Molecules* 2024, 30 (1), 107.
20. Templ, J.; Borchardt, L. Mechanochemical Strategies Applied to the Late-Stage Modifications of Pharmaceutically Active Compounds. *Angew. Chem. Int. Ed.* 2025, e202503061.
21. Osman, A. I.; Chen, Z.; Elgarahy, A. M.; Farghali, M.; Mohamed, I. M.; Priya, A. K.; et al. Membrane technology for energy-saving principles, techniques, applications, challenges, and prospects. *Adv. Energy Sustainability Res.* 2024, 5 (5), 2400011.
22. dos Santos, K. A.; de Carvalho Moreira, L. M. C.; Soares-Sobrinho, J. L.; Soares, M. F. D. L. R. New horizons in antiretroviral drug delivery systems for HIV management. *Curr. Med. Chem.* 2025, 32 (21), 4192–4224.
23. Mallappa; Chahar, M.; Choudhary, N.; Yadav, K. K.; Qasim, M. T.; Zairov, R.; et al. Recent advances in the synthesis of nitrogen-containing heterocyclic compounds via multicomponent reaction and their emerging biological applications: a review. *J. Iran. Chem. Soc.* 2025, 22 (1), 1–33.

24. El-Saghier, A. M.; Enaili, S. S.; Abdou, A.; Hamed, A. M.; Kadry, A. M. Synthesis, docking, and biological evaluation of purine-5-N-isosteres as anti-inflammatory agents. *RSC Adv.* 2024, 14 (25), 17785–17800.

25. Furlong, A. J.; Bond, N. K.; Champagne, S.; Haelssig, J. B.; Symonds, R. T.; Hughes, R. W.; et al. Process Safety Considerations in the Design and Scale-Up of Chemical Looping Processes. *Ind. Eng. Chem. Res.* 2025.

26. Vaz, C. R. S.; Morais, C.; Pastre, J. C.; Júnior, G. G. Teaching Green Chemistry in Higher Education: Contributions to a Problem-Based Learning Proposal for Understanding the Principles of Green Chemistry. *Sustainability* 2025, 17 (5), 2004.

27. Elkanzi, N. A.; Ali, A. M.; Abdelaziz, M. A.; Alishan, A. M. Green synthesis, anti-inflammatory evaluation, and molecular docking of novel pyridines via one-pot multi-component reaction using ultrasonic irradiation. *Mol. Divers.* 2024, 28, 1–11.

28. Vishwakarma, D.; Gupta, S. P. Synthesis, Anti-inflammatory, and in silico Studies of a Few Novel 1, 2, 4-Triazole-Derived Schiff Base Compounds. *Indian J. Pharm. Educ. Res.* 2024, 58 (4), 1235–1241.

29. Paggi, J. M.; Pandit, A.; Dror, R. O. The art and science of molecular docking. *Annu. Rev. Biochem.* 2024, 93 (1), 389–410.

30. Siddiqui, B.; Yadav, C. S.; Akil, M.; Faiyyaz, M.; Khan, A. R.; Ahmad, N.; et al. Artificial intelligence in computer-aided drug design (CADD) tools for the finding of potent biologically active small molecules: Traditional to modern approach. *Comb. Chem. High Throughput Screening* 2025.

31. Ajmal, M.; Mahato, A. K.; Khan, M.; Rawat, S.; Husain, A.; Almalki, E. B., ... & Rashid, M. Significance of Triazole in medicinal chemistry: advancement in drug design, reward, and biological activity. *Chemistry & Biodiversity*, (2024). 21(7), e202400637.

32. Sahu, M. K.; Nayak, A. K.; Hailemeskel, B.; Eyupoglu, O. E. Exploring recent updates on molecular docking: Types, method, application, limitation & prospects. *Int. J. Pharm. Res. Allied Sci.* 2024, 13 (2), 24–40.

33. Mursal, M.; Ahmad, M.; Hussain, S.; Khan, M. F. Navigating the computational seas: a comprehensive overview of molecular docking software in drug discovery. In *Unravelling Molecular Docking—From Theory to Practice*; IntechOpen, 2024.

34. Wu, K.; Karapetyan, E.; Schloss, J.; Vadgama, J.; Wu, Y. Advancements in small molecule drug design: A structural perspective. *Drug Discovery Today* 2023, 28 (10), 103730.

35. Awad, M. A.; Hammad, S. F.; El-Mashtoly, S. F.; El-Deeb, B.; Soliman, H. S. Phytochemical and biological assessment of secondary metabolites isolated from a rhizosphere strain, *Sphingomonas sanguinis* DM, of *Datura* metal. *BMC Complement. Med. There.* 2024, 24 (1), 205.

36. Huang, X.; Li, C.; Zhang, C.; Xiang, Y.; Yu, Z.; Li, P.; et al. Repurposing Etalocib suppresses multidrug-resistant *Staphylococcus aureus* by disrupting the bacterial membrane. *BMC Microbiol.* 2025, 25 (1), 472.

37. Olaiya, V. O. A Study on Antibiotic Susceptibility Pattern of DNase Positive *Staphylococci* Isolated from Selected Libraries of Halls of Residence in Obafemi Awolowo University, Ile-Ife, Osun State, Nigeria. *medRxiv* 2025.

38. Dutta, B.; Das, U.; Ltu, S.; Ghosh, S.; Ray, R. R. Bacteriocin-Mediated Silver Nanoconjugate: Synthesis, Characterization, and Application as an Antibiofilm Agent Against Two Common Pathogenic Bacteria. *Probiotic Antimicrob. Proteins* 2025, 17, 1–20.

39. La Monica, G.; Gallo, A.; Bono, A.; Alamia, F.; Lauria, A.; Alduina, R.; Martorana, A. Novel Antibacterial 4-Piperazinylquinoline Hybrid Derivatives Against *Staphylococcus aureus*: Design, Synthesis, and In Vitro and In Silico Insights. *Molecules* 2024, 30 (1), 28.

40. Asaftei, M.; Lucidi, M.; Anton, S. R.; Trompeta, A. F.; Hristu, R.; Tranca, D. E.; et al. Antibacterial interactions of ethanol-dispersed multiwalled carbon nanotubes with *Staphylococcus aureus* and *Pseudomonas aeruginosa*. *ACS Omega* 2024, 9 (31), 33751–33764.

41. Kader, D. A.; Aziz, D. M.; Mohammed, S. J.; Maarof, N. N.; Karim, W. O.; Mohamad, S. A.; et al. Green synthesis of ZnO/catechin nanocomposite: Comprehensive characterization, optical study, computational analysis, biological applications, and molecular docking. *Mater. Chem. Phys.* 2024, 319, 129408.

42. Oberbauer, V.; Mutti, M.; Schwebs, T.; Durica-Mitic, S.; Visram, Z.; Kestemont, D.; et al. Discovery of potent endolysins against *Pseudomonas aeruginosa* and other gram-negative ESKAPE pathogens by an agar-based screening method. *Sci. Rep.* 2025, 15 (1), 29351.

43. Breijyeh, Z.; Karaman, R. Design and synthesis of novel antimicrobial agents. *Antibiotics* 2023, 12 (3), 628.

44. Mohammed, I. A.; Al-Assafe, A. Y.; Fathi, A. A. *Bull. Chem. Soc. Ethiop.* 2025, 39, 841–857.

45. Synthesis, structural characterization, and biological activity of novel Schiff-base complexes incorporating... *Bull. Chem. Soc. Ethiop.* 2024, 38 (2), 325–346.

46. Rafiq, M. A.; Shahid, M.; Jilani, K.; Aslam, M. A. Antibacterial, antibiofilm, and anti-quorum sensing potential of novel synthetic compounds against pathogenic bacteria isolated from chronic sinusitis patients. *Dose-Response* 2022, 20 (4), 15593258221135731.

47. Flores, D.; Jerves, C. Computational Comparison of the Binding Affinity of Selective and Nonselective NSAIDs to COX-2 Using Molecular Docking. *Bionatura J* 2025, 2 (3).

48. Bello-Vargas, E.; Leyva-Peralta, M. A.; Gómez-Sandoval, Z.; Ordóñez, M.; Razo-Hernández, R. S. A computational method for the binding mode prediction of COX-1 and COX-2 inhibitors: analyzing the union of coxibs, oxicams, and propionic and acetic acids. *Pharmaceuticals* 2023, 16 (12), 1688.

49. Nagham Majid Abdulhassan; Abdul Jabar Kh. Atia; Falah S. Al-Fartusie. Design, Synthesis, and in Vitro Biological Activity of Five- and Six-Membered Heterocycles Naproxen Derivatives. *Appl. Chem. Eng.* 2025, 8, ACE-5740.
50. Hameed, A. N., Atia, A. J. K., & Al Jorani, K. R. Synthesis and Biological Activity of New Heterocyclic Compounds Derived From N-Benzoylthioimidazolidin-4-one. *Solid State Technology*, (2020) 63(6), 1080-10821
51. Dadoosh SA, Mahdi MF, Atia AJK. Synthesis, characterization, and antibacterial study of some imidazole and molecular docking of new heterocyclics from furan derivatives. *Journal of Biochemical Technology*. 2019; 10(4-2019): 76-81
52. Abdulnabi AA, Ali KF, Abd Razik BM. Synthesis, Characterization, ADME Study, and Antimicrobial Evaluation of New 1, 2, 3-Triazole Derivatives of 2-Phenyl Benzimidazole. *Al Mustansiriyah Journal of Pharmaceutical Sciences*. 2023; 23(2): 147-57.